Synthesis, Characterization, and Dynamics of a Rod/Sphere Composite Liquid

Mark A. Tracy and R. Pecora*

Department of Chemistry, Stanford University, Stanford, California 94305-5080

Received July 22, 1991; Revised Manuscript Received September 13, 1991

ABSTRACT: A new rod/sphere composite liquid was synthesized, characterized, and studied by dynamic light scattering (DLS). The liquid consists of coated silica spheres and poly(γ-benzyl-α,L-glutamate) rods (PBLG) in dimethylformamide (DMF). Diffusion constants for spheres of radius 60.4 nm and PBLG rods of length 70 nm were measured by DLS in binary sphere/DMF and rod/DMF solutions as functions of concentration. The diffusion in the binary solutions is compared to that in ternary sphere/rod/DMF solutions at similar sphere and rod concentrations. These studies show that the diffusion of each species in the composite liquid can be measured simultaneously. No evidence was found for aggregation in either the binary or the ternary solutions. Changing the solvent to a mixture of DMF and pyridine allowed the spheres to be refractive index matched to the solvent, greatly decreasing their light scattering intensity. The diffusion of the rods in the composite liquid consisting of dilute spheres and rods of varying concentration was essentially the same as that in the binary rod/DMF solution. The transition between dilute and semidilute rod behavior was found to fall at 8.4 mg/mL or $nL^3 = 17$, in the middle of the concentration range studied ($2 < nL^3 < 60.4$). This value is similar to that found by Zero and Pecora for PBLG in dichloroethane. As the rod concentration increases, the product of the sphere diffusion constant and the solution viscosity remains constant, indicating that the sphere diffusion is consistent with the Stokes-Einstein equation. The dependences of the sphere diffusion constant and the solution viscosity on the rod concentration are well fit by a stretched exponential: $D/D_0 = \eta_0/\eta = \exp(-0.16c^{0.81})$. The $c^{0.81}$ dependence is comparable to that found from experiments using flexible coils as the background polymer. Theoretical predictions for rods, however, give a $c^{0.5}$ dependence. The similar concentration dependence for silica spheres found in rod and coil solutions suggests that polymer flexibility alone does not account for the deviation from the theoretical $c^{0.5}$ predictions. Instead, rod-rod hydrodynamic interactions may play an important role in this deviation.

I. Introduction

There has in recent years been a growing interest in the study of liquid dispersions consisting of particles, macromolecules, and solvents, primarily because of their technological importance.[1] Examples of these so-called composite liquids include ceramic precursors, lubricants, paints, adhesives, and the cytoplasm in biological cells. Due to the complexity of these liquids, experimental studies of precisely defined systems are essential in developing an understanding of the interactions between all components in the liquid. A primary technique for measuring the dynamics of complex systems is dynamic light scattering (DLS). DLS is noninvasive and can, at least in principle, measure the diffusion of both the particle and macromolecular species in a complex liquid mixture simultaneously. Unfortunately, it is quite difficult in practice to prepare composite liquids that take full advantage of the capabilities of DLS. In the most important composite liquids, the particles are usually spheres. In most systems studied to date the sphere scattering dominates that of the macromolecule so that macromolecule and sphere diffusion cannot be measured simultaneously. Other complications (common to all measurement techniques) include adsorption of the macromolecule onto the sphere and aggregation. Despite these limitations, DLS has, nonetheless, been used to study aqueous solutions of polystyrene spheres and flexible or semiflexible macromolecules[2-14] largely because these solutions are relatively easy to prepare. Only the sphere diffusion could be studied in most cases.

Recently, Zhou and Brown[15] and Rymdén and Brown[16] were able to overcome the above-mentioned obstacles. They prepared silica sphere/polyisobutylene and silica sphere/poly(methyl methacrylate) coil solutions and measured the diffusion constants of the sphere and the coil simultaneously using DLS. Still, however, a precisely defined sphere/rigid rod polymer composite liquid has not, until now, been prepared and systematically studied. Rigid or semirigid rodlike macromolecules are important constituents of composite liquids. They are, for instance, often used as viscosity enhancers. In this article we discuss the preparation, characterization, and dynamics of a new model composite liquid consisting of silica spheres and poly(γ-benzyl-α,L-glutamate) (PBLG) rigid rods in dimethylformamide (DMF).

There are five main goals of this study: (1) the synthesis of a rod/sphere liquid free from adsorption and aggregation complications, (2) the simultaneous measurement of the diffusion constants of the rods and the spheres at a variety of concentrations of both species, (3) the ability to vary the scattering power of the strongly scattering spheres so the diffusion of both species can be measured at higher sphere concentrations, (4) the comparison of the diffusion behavior of both rods and spheres in the ternary system to binary rod/solvent and sphere/solvent solutions, and (5) the comparison of sphere diffusion through rods to data on sphere diffusion through other kinds of polymers in other solvent environments. Is sphere diffusion a Stokes-Einstein process which depends only on the viscosity of the solvent and the sphere radius? Are the measured diffusion constants consistent with the theoretical scaling laws that predict the diffusion constant's dependence on rod concentration?

II. Synthesis

The first objective of the rod/sphere liquid synthesis was to prepare a simple system that could be used to study the dynamics at a wide variety of rod and sphere concentrations. The silica/PBLG/DMF system meets this objective. Both silica and PBLG are dispersible as singlets in DMF. This is also one of the few solvents in which PBLG is rodlike. Others are pyridine, *m*-cresol, and 1,2-dichloroethane. The spheres can be synthesized to any size from a few tens of nanometers to almost 1 μm in diameter.

0024-9297/92/2225-0337$03.00/0

The rods also can be obtained in a variety of molecular weights. Thus, the spheres and rods are capable of being sized so their diffusion constants are resolvable using DLS over wide concentration ranges. In addition, an optical refractive index matching procedure was developed using a pyridine/DMF mixed solvent that enables the dynamics of both the rods and spheres to be measured even at moderate sphere concentrations (concentrations at which in DMF alone the sphere scattering dominates).

Sphere Preparation. The spheres were synthesized by the method of Stöber et al.[17,18] The reaction was performed in absolute ethanol (EtOH) that was dehydrated by adding 5 g of magnesium turnings and 5 mL of CCl_4 before refluxing and distilling. The tetraethylorthosilicate (TEOS) (Aldrich Chemical Co., electronic grade) was vacuum distilled before use. Ammonium hydroxide (J. T. Baker and Co., 30%) was used as received. Titrations indicated an ammonia concentration of 14.6 M. Distilled, deionized water was also used. Seed particles of hydrodynamic radius 40.5 nm, determined by DLS, were grown from a solution of 0.18 M TEOS, 0.80 M NH_3, and 1.99 M H_2O at 40 °C. These particles were grown to a final radius of 60.2 ± 0.8 nm using the seeded growth procedure of Bogush et al.[19] This procedure was used to increase the solids content of the sol from 1.0% to 4.7%. Four 20-mL doses of TEOS were required to reach the final size. The water content of the sol was carefully calculated before each TEOS dose. A minimal amount of water was added as necessary to insure that there was just enough present to react completely with the TEOS.

Coating Procedure. The spheres were then coated with the silane coupling agent 3-(trimethoxysilyl)propyl methacrylate (TPM) ($H_2C{=}C(CH_3)COO(CH_2)_3Si(OCH_3)_3$). Once coated the spheres were dispersible in a variety of polar organic solvents in which PBLG is rodlike and nonaggregating. These solvents include DMF, pyridine, *m*-cresol, and 1,2-dichloroethane.[20]

The coating procedure was based on that of Philipse and Vrij.[21] First, the water content of the sol was measured by a Karl–Fischer titration. The water content of the final sol was 2.8%, well below the azeotropic H_2O/EtOH composition of 4% H_2O. This step is critical because water must be removed from the solution in order to promote the condensation of TPM to the silica surface. If the water composition is above 4%, the sol must be totally dried before condensation can begin. But if the water content is below 4%, then only a simple distillation is needed to remove the water. The distillation avoids heating silica in the dry state, which often causes irreversible aggregation. So if it turned out that the water content was above 4%, absolute ethanol was added to reduce it below this value. In addition, the exposure of the sol to air was minimized as a further precaution against unneeded water entering the system. The sol was stored in an Aldrich Atmosbag containing desiccant and purged periodically with argon.

The amount of TPM added to the sol was estimated from the number of particles per unit volume of alcosol, the surface area per particle, and data of Philipse and Vrij.[21] The number of particles was determined in the initial growth stage. Further seeded growth steps merely increased the size of the particles but did not cause additional particle nucleation.[19] The number of particles per unit volume of sol (N_p)

$$N_p = c_i/(\rho_p * V_p) \tag{1}$$

was calculated from the total amount of SiO_2 (c_i(g/L)) in the alcosol after the initial growth stage, the density of the particles (ρ_p), and the volume of one spherical particle (V_p), where $V_p = {}^4/_3\pi R^3$. The particle radius R was equated to the hydrodynamic radius and was determined by DLS on a diluted sample of the sol taken after the first growth step.

The amount of TPM to add should be proportional to the surface area per particle ($4\pi R^2$) after the final growth step. Thus, if ρ_p does not change, the amount of TPM to add to adequately coat the spheres under conditions 2 may be estimated in terms of that found to be successful under conditions 1 by

$$\frac{[\mathrm{TPM}]_1}{[\mathrm{TPM}]_2} = \frac{[\mathrm{TEOS}]_{1i}}{[\mathrm{TEOS}]_{2i}}\left(\frac{R_{2i}}{R_{1i}}\right)^3\left(\frac{R_{1f}}{R_{2f}}\right)^2 \tag{2}$$

where i refers to the concentrations and particle radii after the initial growth step, and f refers to the particle radius after the final growth step.

Conditions 1 were determined by Philipse and Vrij: $[\mathrm{TPM}]_1$ = 0.117 M, $[\mathrm{TEOS}]_{1i}$ = 0.265 M, R_{1i} = 51.3 nm, R_{1f} = 74.0 nm. For the sol discussed here, R_{2i} = 40.5 nm, R_{2f} = 60.4 nm, $[\mathrm{TEOS}]_{2i}$ = 0.179 M, so that $[\mathrm{TPM}]_2$ = 0.107 M. Estimates from eq 2 were used to successfully coat silica spheres varying in radius from 40 to 160 nm. Tests indicated that even adding 50% less TPM than the formula's estimate was enough to coat the spheres so that they were dispersible as singlets in DMF. Further studies are required to determine the precision of this formula's predictions. It should be noted that no other such predictions have been found in the limited literature on coating particles with silane coupling agents.[22]

After adding the TPM to the alcosol, the mixture was stirred for 50 min at ambient temperature (23.5 °C) in a stoppered round-bottom flask. This hydrolyzed the methoxy groups on the TPM. The reaction mixture was heated slowly to the boiling point with magnetic stirring. Then, 136 mL of solution was distilled off under anhydrous conditions. This took 4 h. The maximum temperature of the glycerol heating bath was 94 °C. Enhanced stability in ethanol/toluene mixtures confirmed the presence of TPM on the silica particles. The sol contained 6.1% silica. The alcosol was further concentrated by vacuum distillation. A 106-mL portion of distillate was collected. The coated particle radius in ethanol was measured to be 61.9 nm by dynamic light scattering. The DLS results showed no evidence of aggregates. Since the bare spheres have a radius of 60.2 nm, the coating is about 1.7 nm thick in ethanol solvent.

Solvent Replacement. The ethanol was then replaced by dimethylformamide (DMF) (Aldrich, HPLC Grade) because PBLG is rodlike and nonassociating in DMF. This was done by adding DMF as received to the alcosol and distilling off the ethanol under reduced pressure. These two solvents were completely miscible at the compositions used and did not form an azeotrope. Enough DMF was added to give a 70% DMF sol. The temperature of the bath was kept cooler than 60 °C to minimize particle clustering on the hot flask surface. The pressure was reduced to 100 kPa of vacuum. The sol was distilled for 5 h, long enough to insure that the distillate volume was much greater than the original volume of the sol before adding DMF (334 mL). After the distillation was stopped, the sol was placed in a brown glass bottle. The outside of the bottle was covered with aluminum foil to minimize exposure of the coating to UV light, which may cause it to polymerize.[21] A few residual flocs remained at the bottom of the distillation flask, but DLS experiments showed the sol was free of any aggregates. A 4.0-mL sample of the sol was placed in a glass centrifuge tube opened to the air at 20 °C and centrifuged for 24 h at a relative centrifugal force ($=\omega r^2/g$) of 1247 along with a tube of pure DMF. The index of refraction of the sol supernatant as measured by an Abbe refractometer differed from that of the pure DMF by less than 0.1%. Thus, the supernatant was almost pure DMF. The density of the sol was 0.97 ± 0.01 g/mL. The silica content of the sol was determined by drying a few milliliters of the sol for 3 days at 80 °C, including 4 h under 100 kPa of vacuum. The mass percent of silica in the sol was 5.54 ± 0.06%. The coated particle radius in DMF was found to be 60.4 ± 0.4 nm from DLS experiments. A 0.019% silica/DMF solution was used in this experiment.

Rod Characterization. The PBLG ($-(COCH(CH_2)_2COOCH_2C_6H_5HN)_n-$) was purchased from Sigma Chemical Co. (Lot #28F50171) and used as received. The weight average molecular weight, M, was determined to be 102 000 ± 2000 g/mol in DMF by total intensity light scattering (see below). A viscosity average molecular weight of 125 000 g/mol and a weight average value of 105 600 were reported by Sigma. The radius of gyration, r_g, also determined by total intensity light scattering as described below, was 19 ± 3 nm.

The total intensity apparatus used was constructed in our laboratory (Figure 1). Incident 488-nm laser light from a Spectra-Physics Series 2000 Ar^+ laser was focused into a 1.0-cm path length Spectrocell light scattering cuvette. To reduce stray light and regulate the sample temperature, the cell was placed in a Brookhaven Instruments Co. BI-TCA index-matching bath with temperature control identical to the one used in the DLS experiments. The scattered light was collected at four angles.

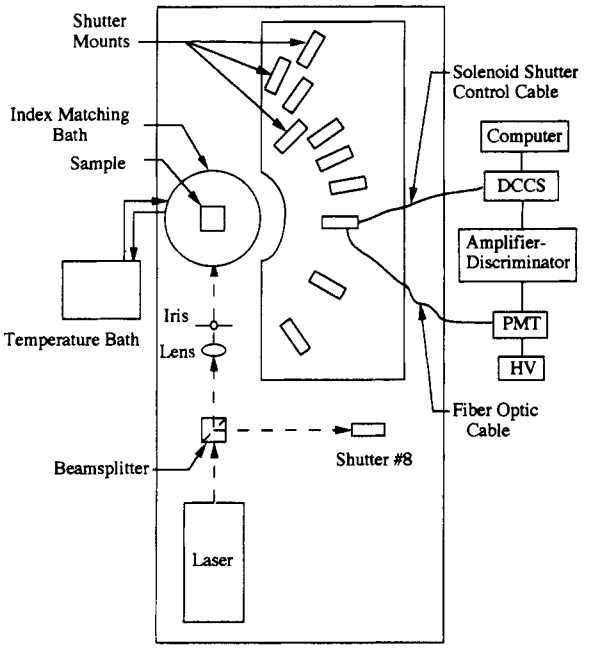

Figure 1. Schematic of the total intensity light scattering apparatus. The DCCS is the data collection and control system (see the text), PMT is the photomultiplier tube, and HV the high-voltage source for the PMT. The apparatus is mounted on an optical table.

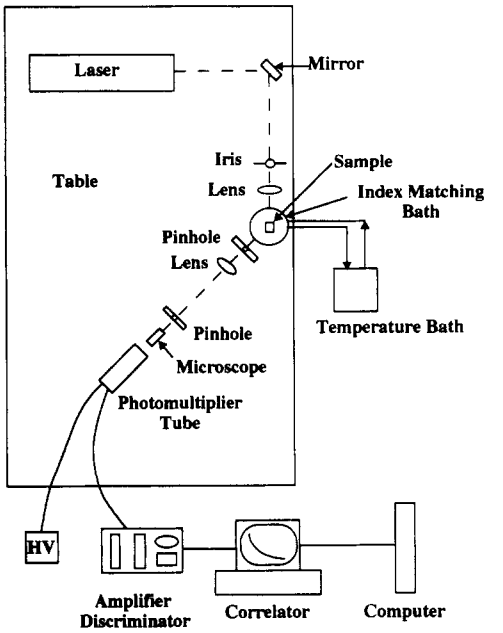

Figure 2. Schematic of the dynamic light scattering apparatus.

At each angle a lens focused the light into a fiber optic cable connected to an EMI 9205-RF photomultiplier tube (PMT) mounted in a refrigerated enclosure. There was a timer-driven shutter between the lens and the cable to insure that all channels received scattered light for the same amount of time. One channel (channel 8) was used to monitor the beam stability. The shutters were controlled by a specially built data collection and control system (DCCS). The DCCS also counted the incoming digitized pulses from the photomultiplier tube and the amplifier–discriminator. The data was stored in a computer for further analysis.

The intensity of the scattered light was measured at scattering angles θ of 39.01°, 58.90°, 74.97°, and 97.45°. Before measurement, the samples were centrifuged for 2 h. The total intensity, i_{sample}, was calculated relative to the intensity of toluene, which was determined after that for each polymer sample. The intensities were related to the Rayleigh ratio by

$$R_\theta/R_{\theta tol} = i_{sample}/i_{toluene} \tag{3}$$

For toluene, $R_\theta = 3.96 \times 10^{-5}$ cm^{-1} at 488 nm and 25 °C.[23] If an intensity value deviated by more than 10 standard deviations from the mean, the point was rejected. The dust-corrected results differed from the uncorrected results by at most 2%. A Zimm plot was made from dust-corrected data and interpeted using eq 4 for linearly polarized incident light:[23]

$$\left(\frac{Kc}{R_\theta}\right)_{c=0} = \frac{1}{M}\left(1 + \frac{16\pi^2 n^2}{3\lambda_0^2} r_g^2 \sin^2\left(\frac{\theta}{2}\right)\right) \tag{4a}$$

where the optical constant is given terms of the solution refractive index, n, the wavelength of light, λ_0, and Avogadro's number, N_a, by

$$K = \frac{4\pi^2 n^2}{\lambda_0^4 N_a}\left(\frac{dn}{dc}\right)^2 \tag{4b}$$

Composite Liquid Preparation. The PBLG was dried at 35 °C for 2 h under vacuum before it was further used. The proper amount of PBLG was then added to a weighed, dry volumetric flask. It is important that the volumetric flask be dry because the PBLG/DMF system undergoes phase separation in the presence of water.[24] The flask with PBLG was weighed again to determine the amount of PBLG present. Most of the solvent was then added and the solution was shaken and hand-warmed until the polymer was fully dissolved. The required amount of the silica sol was added and then the solution was diluted to the mark with pure solvent if necessary. Each composite liquid was allowed to equilibrate at least 1 day before being filtered into Spectrocell quartz light scattering cuvettes. Up to 1 week was allowed for the most concentrated polymer solutions to equilibrate.

III. DLS Measurements

The following procedure was used to filter the composite liquid and polymer solutions into the 1.0-cm quartz light scattering cuvettes. The cuvettes were made dust-free by first filtering deionized, distilled water into the cell overnight using a Sage Instruments Model 375A peristaltic pump. A Millipore Millex-GS 0.22-μm filter was used. Then about 20–30 mL of absolute ethanol followed by the same amount of solvent was filtered into the cell using a 50-mL glass syringe and a 0.2-μm Millipore Fluoropore FG filter. The cells were placed in the laser beam and checked for dust using a ×5 microscope. Before the sample was added, a 0.5-μm Millipore Fluoropore FH filter was dipped in absolute ethanol to wet its surface. About 10 mL of pure DMF were passed through the new filter to remove any remaining residues. Then a clean and dry 5-mL glass syringe was filled with the sample. Finally, the sample was filtered into the clean, dust-free cuvette. The cuvette was rinsed with a few tenths of a milliliter of sample before adding the final amount to the cuvette. After the final amount of sample was added, the cuvette was quickly sealed and stored in a desiccator. Again at least 1 day was allowed for equilibration. All leftover solutions were stored in the Aldrich Atmosbag containing desiccant.

The DLS apparatus used (Figure 2) was assembled on two Newport Research Co. optical rails. The first was mounted along the edge of a hemispherical steel plate with holes drilled at 5° intervals around its circumference. The other rail was anchored to the first by a brass pin at the pivot point. This rail was free to move 130° about the pivot point. The 488-nm line of a 5-W Spectra-Physics Model 165 Ar^+ laser served as the light source for all the experiments. The beam was guided down the center of the fixed optics rail by a coated mirror. A 200 mm focal length lens and an iris were used to focus the beam into the scattering cell. To minimize stray light and regulate

Table I
Sample Concentrations

A. Rod/DMF Solutions

rod concn, mg/mL	ξ_c, nm	ξ_r, nm	ξ_s, nm	ξ_h, nm	nL^3 ($n = cN_a/M$)
1.1	55.4	145	11.2	9.86	2.0
3.2	37.6	50.2		9.93	6.4
5.0	32.4	32.0	6.86	10.1	10.1
7.54	28.2	21.2		10.1	15.2
10.0	25.7	16.0	7.61	9.78	20.2
15.0	22.4	10.6		9.16	30.4
20.9	20.1	7.64	3.40	8.34	42.3
30.2	17.8	5.28		7.82	61.1

B. Rod/Sphere/DMF Solutions

rod concn, mg/mL	sphere concn		N_pR^3 [a] ($\times 10^5$)
	mg/mL	mass %	
1.0	0.0472	0.005	0.70
3.2	0.0944	0.010	1.4
5.0	0.0472	0.005	0.70
10.0	0.0472	0.005	0.70
15.1	0.142	0.015	2.1
20.9	0.0944	0.010	1.4
29.9	0.283	0.030	4.2

[a] N_p is the sphere number concentration (eq 1).

the sample temperature, the cell was centered in a Brookhaven Instruments Co. BI-TCA index-matching bath with temperature control. The index fluid used was a hydrocarbon mixture (#4550) produced by R.P. Cargille Laboratories. It has an index of refraction of 1.452 at 589.3 nm and 1.4575 at 488 nm and 25 °C. The fluid was filtered for 1 or 2 min before each sample was inserted. Temperature-controlled water was pumped through a copper coil around the bath by a Lauda K-2/R circulating bath. The temperature was controlled to ±0.1 °C.

The analyzing optics were all mounted on the pivoting optics rail. The scattered light first passed through a 500-μm pinhole and was focused by a 100 mm focal length lens onto a 200-μm pinhole. This was followed by a microscope with a beam splitter that both focused the scattered light onto the PMT cathode and diverted some of the light into an eyepiece so the scattering volume could be observed. The PMT was a Thorn EMI 9893A/350 selected for low afterpulsing and dark count. The dark count was 10 cps at 1965 V. The tube signal was amplified by an EG&G Ortec Model 9301 fast preamplifier located just after the PMT. The output then went to an EG&G Ortec 9302 amplifier–discriminator followed by an EG&G Ortec 994 counter–timer. TTL pulses were sent to a Brookhaven Instruments Model 2030AT 136 data + 6 delay channel correlator. The correlation function was displayed on a monitor and stored in an IBM PC AT. The data were sent to a Digital Equipment Co. Vaxstation 3200 computer for analysis.

The composite liquid solution concentrations studied are shown in Table I. Binary solution dynamics were also measured. Sphere diffusion in DMF was measured at silica concentrations from 0.094 to 4.7 mg/mL (0.01–0.50 mass %). PBLG diffusion in DMF was measured at rod concentrations from 1.0 to 30.2 mg/mL (0.10–3.2 mass %). DLS data were taken at a minimum of three of the following angles: 25.45° or 30.56°, 59.44°, 90°, and 110.35° or 120.56°. All experiments were done at 25 °C. The laser power varied between 20 and 800 mW. Data were collected for between 3 min and 3 h, depending on sample concentrations and measurement angle.

Solution viscosities were measured in an Ostwald capillary viscometer in a water bath at 25.0 ± 0.1 °C. The viscosities of the composite liquid samples after filtering were on average 3% lower than the viscosities of the unfiltered samples. Thus, there was probably some polymer loss upon filtration but not enough to affect the results. Ultraviolet analysis for PBLG in DMF is not possible because their signature peaks overlap. Since the light scattering samples were filtered, the viscosities of the filtered solutions were taken as the correct ones.

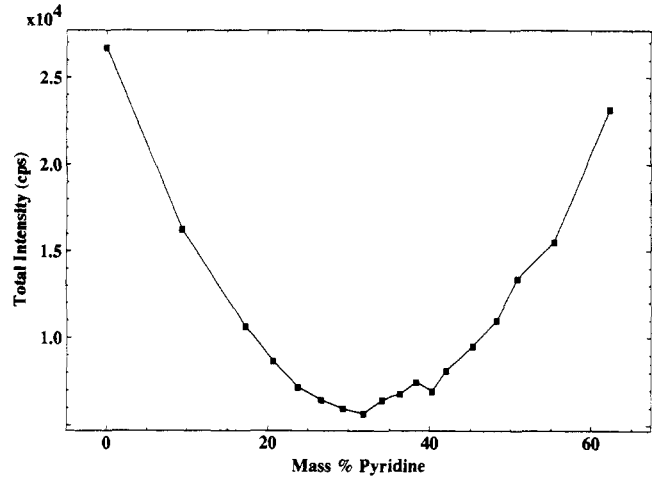

Figure 3. Variation in scattered light intensity measured at 90° in counts per second as a 0.005% silica/pyridine solution was added to a 0.005% silica/DMF solution. The minimum is at 31.8% pyridine.

Samples sealed in light scattering cuvettes were stable for at least 1 year. Since there was evidence of evaporation over such extended periods of time, it is best to perform measurements within 1–2 weeks after samples are prepared.

Refractive Index Matching Point Determination. Pyridine was chosen to be used along with DMF in the sphere-matching study. It was selected over the other possibilities like *m*-cresol and dichloroethane because, in addition to having a quite different index of refraction from DMF, it is completely miscible in DMF and its viscosity, density, and other relevant solvent properties are similar.

To find the pyridine/DMF matching composition for dilute solutions of silica spheres, two solutions of constant sphere composition were made. The first contained 0.005% silica and DMF. The second consisted of 0.005% silica, 0.008% DMF (from the silica/DMF sol), and pyridine. First, 1.00 mL of DMF/silica was added to a clean dust-free light-scattering cuvette. Then the unfiltered pyridine/silica solution was added in 10 0.1-mL increments followed by 2 increments greater than 0.1 mL. The sphere composition was kept constant at all times because the silica concentration in both solutions was the same. After each addition, the cell was lightly shaken and placed in the DLS apparatus. The absolute intensity in counts/second was measured for the sample at 90°. Thirty or more values of the intensity were recorded and averaged to obtain an average scattered intensity of the spheres at each solvent composition from 100% DMF to 60% pyridine. The average scattered intensity reached a minimum at 31.8% pyridine (Figure 3). At this point the scattered intensity was nearly equal to the background intensity without the sample. Later DLS experiments on clean samples verified that this was indeed the matching composition.

Data Analysis. The autocorrelation function $C(\tau)$ that is measured in the DLS experiments is proportional to the homodyne autocorrelation function $I_2(\tau)$. If the Gauss-

ian approximation holds, this correlation function reduces to[25]

$$C(\tau) = B[1 + A|I_1(\tau)|^2/|I_1(0)|^2] \quad (5)$$

where $|I_1(\tau)|^2/|I_1(0)|^2 \equiv g_1^2(\tau)$ is the square of the normalized scattered electric field autocorrelation function, and B is the baseline. The baseline can either be calculated from the total number of counts that arrive during the duration of an experiment or obtained from the measured correlation function at long correlation times τ.[26] A is a constant that depends on the scattering geometry and is determined by a fit to the data. Sample correlation functions are shown in Figure 4.

By fitting $C(\tau)$ to model predictions for $g_1(\tau)$, diffusion constants are determined. For simple systems of small, monodisperse particles undergoing Brownian diffusion, $g_1(\tau)$ is modeled as a single exponential decay.

$$g_1(\tau) = \exp(-\tau/\tau_R) \quad (6)$$

where $\tau_R = 1/q^2D = 1/\Gamma$ is the decay time of the particle. D is its diffusion constant and q is the magnitude of the scattering vector length given by $q = (4\pi n/\lambda_0) \sin(\theta/2)$.

For dilute dispersions of noninteracting spheres, the diffusion coefficient is related to the sphere hydrodynamic radius R_h by the Stokes–Einstein relation:

$$D = kT/6\pi\eta R_h \quad (7)$$

where k is the Boltzmann constant, T is the absolute temperature, and η is the solution viscosity.

For dilute, long, thin, rigid rods, Broersma gives the following for $L/d > 5$:[27-29]

$$D = (kT/3\pi\eta_0 L)[\delta - (1/2)(\gamma_\parallel + \gamma_\perp)] \quad (8)$$

where

$$\delta = \ln(2L/d) \qquad \gamma_\parallel = 1.27 - 7.4(1/\delta - 0.34)^2$$
$$\gamma_\perp = 0.19 - 4.2(1/\delta - 0.39)^2$$

and η_0 is the solvent viscosity. For shorter rods, Tirado and Garcia de la Torre give the following for $2 < L/d < 30$:[30]

$$D = (kT/3\pi\eta_0 L)[\ln p + \nu] \quad (9)$$

where

$$p = L/d \quad \text{and} \quad \nu = 0.312 + 0.565p^{-1} - 0.100p^{-2}$$

For multicomponent or polydisperse systems, $g_1(\tau)$ can be modeled as a weighted sum of exponential decays.

$$g_1(\tau) = \int_0^\infty G(1/\tau_R) \exp(-\tau/\tau_R)\, d(1/\tau_R) \quad (10)$$

Two methods of analysis were used in this study to determine the distribution of decay times $G(1/\tau_R)$ leading to the correlation function decay. These are the method of cumulants[31] and the FORTRAN program CONTIN.[32-33] The method of cumulants is the simplest of the two. A weighted average diffusion constant can be calculated from the first cumulant (K_1) and a measure of the broadness of the distribution or polydispersity can be determined from the second cumulant (K_2) if normalized by K_1^2. This method is most useful for distributions that are not too broad. In this study, the method of cumulants was as good as any in analyzing the binary rod/DMF and sphere/DMF data, but it was not effective in handling the composite liquid data. Data was fit up to the second cumulant.

CONTIN is capable of analyzing more complex data than the method of cumulants because it calculates the whole distribution of decay times and not merely the overall

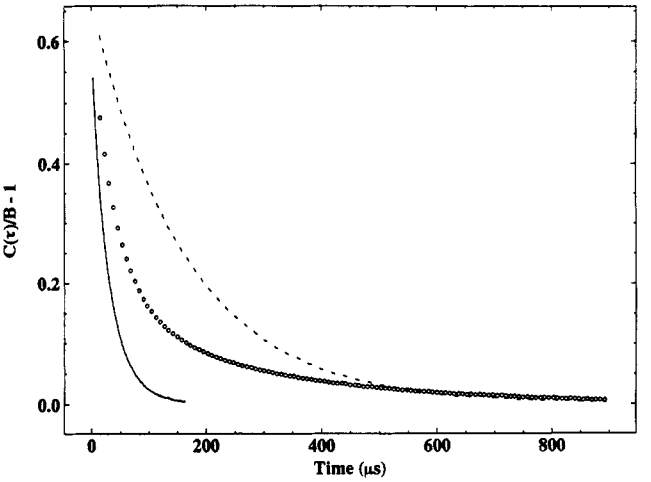

Figure 4. Sample correlation functions measured at 90°: Dashed curve, 0.01% spheres in DMF; solid curve, 0.5% rods in DMF; dotted (O) curve, 0.005%/0.5% sphere/rod mixture in DMF.

average and width of the distribution. The program obtains $G(1/\tau_R)$ by performing an inverse Laplace transform on eq 10. This is however an ill-posed problem because there are an infinite number of solutions that fit the data within its precision. The program overcomes this problem by a constrained regularization (smoothing) method in which the program uses statistical criteria to determine the simplest distribution (fewest number of peaks) consistent with the data. As a result CONTIN, unlike most other methods like DISCRETE, does not require the number of exponentials or peaks of the distribution to be input in advance. Because CONTIN seeks the smoothest solution, it is a conservative method that will ordinarily not overestimate the number of relaxation processes occurring in the system. All data here were analyzed by version 2 of CONTIN over any range (window) of decay times deemed appropriate by the user.

Using CONTIN when there is one dominant relaxation process is straightforward. The program is also good at handling multimodal systems, but more data sets are usually required to obtain the degree of precision in the values of the diffusion constants found for monomodal distributions. For example, between 10 and 44 data sets were analyzed for each composite liquid sample. The diffusion constants of the rods and the spheres were determined to a standard deviation of 4–6%. However, only 9–17 data sets were analyzed for the rod/DMF solutions and a precision of 1–2% was obtained in the rod diffusion constant. The results were similar for sphere/DMF solutions.

Because of the bimodal nature of the decay time distribution, taking data for each composite liquid sample and analyzing it was more complicated and time consuming than for the binary solutions. As already mentioned, more data sets were taken. The main reason for this was that the proper sample times were more difficult to pinpoint. As a result, for each solution the sample time at each angle was varied by between a factor of 2–3. The minimum sample times were chosen such that the difference between the measured and calculated baselines was always less than 0.5%. At the shorter sample times, the fast decay (rod) was better resolved than at the longer sample times. In fact, for the solutions with the highest polymer concentrations, the fast process decayed to 37% of its maximum in as few as 10 channels at the longest sample times. Consequently, CONTIN could resolve it only as a very broad peak often reaching the fast decay time edge

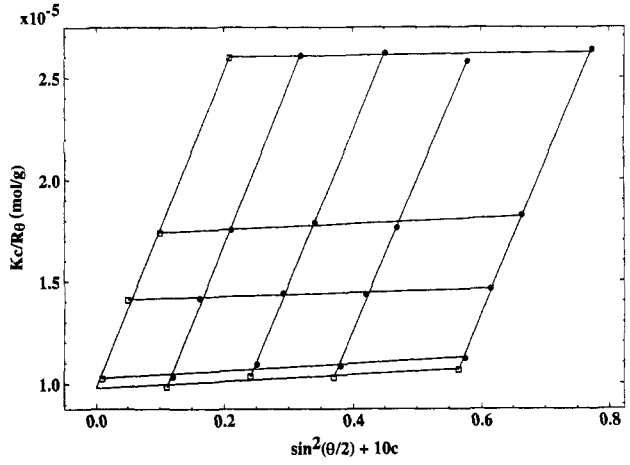

Figure 5. Zimm plot for PBLG in DMF: ●, experimental data; □ extrapolations to $\theta = 0$ and $c = 0$.

of the window. Fortunately, the slow (sphere) peak position did not vary over the range of sample times used so most of the data were taken at sample times where the fast peak could be well resolved.

After analyzing the data with CONTIN, the diffusion constants corresponding to each peak were averaged with other data taken for the same sample at the same angle. Then, Γ vs q^2 plots were used to determine if the diffusion process was angularly independent. If it was, the average diffusion constant was determined from the slope of the linear plots. Several criteria were established for neglecting data. If a diffusion constant was quite different from the average, Chauvenet's criterion was used to determine if it should be neglected. Chauvenet's criterion provides a statistical basis for rejecting improbable data. It states that if the expected number of measurements at least as bad as the suspected measurement is less than 0.5, then the suspect measurement should be rejected.[34] Also, data were not used if the mean peak(s) followed the end of the decay time window as it was varied. Finally, a few sets were eliminated because they exhibited a different number of peaks from the bulk of the data. In most of these sets, it was clear CONTIN was having an unusual degree of difficulty fitting the fast peak and, as a result, split it into two peaks. The diffusion constants in many of these sets also failed Chauvenet's criterion. In any event, for any given sample no more than 10% of the data were rejected. The key to understanding how CONTIN handles multimodal correlation functions is to take a large number of data sets at several angles.

IV. Binary System Results

Rod/Solvent Studies. Total Intensity Light Scattering. The total intensity light scattering results for PBLG are shown in the Zimm plot (Figure 5). The differential index of refraction was taken to be 0.118 ± 0.002 mL/g at 488 nm.[35] The weight average molecular weight is 102 000 ± 2000 g/mol. The thermodynamic second virial coefficient A_2 extracted from the data is (3.9 ± 0.1) × 10^{-4} cm^3mol/g^2 and the radius of gyration (r_g) is 19 ± 3 nm. The errors were determined from the uncertainty in the least-squares fit of the data extrapolated to $\theta = 0°$ and $c = 0$, respectively. The error in r_g is large because the rod is small, so the slope of the $c = 0$ line in the Zimm plot is small. If the PBLG is a rod, the radius of gyration predicts a rod length of 67 ± 10 nm. This compares well to the length of 70 ± 1 nm calculated from the molecular weight, the length per monomer of 0.15 nm,[36] and the molecular weight of the monomer (219 g/mol). This agreement indicates that PBLG of this molecular weight is quite stiff in DMF. There was no evidence for aggregation in the total intensity light scattering experiments.

The geometric (as contrasted with the hydrodynamic) diameter of the rods was calculated from the second virial coefficient using the theories for A_2 for hard rods of Zimm, Onsager, and Schulz (ZOS) (eq 11), and Ishihara (eq 12),[37]

$$A_2 = \pi N_a d L^2/4M^2 \tag{11}$$

$$A_2 = (4N_a v_m/M^2)f,\ f = {}^1/_4[1 + (L/d)(1 + d/2L)(1 + \pi d/2L)] \tag{12}$$

where, for cylinders, $v_m = \pi d^2 L/4$. Thus, if $L \gg d$, eq 12 reduces to eq 11.

A geometric diameter of 1.75 nm was calculated using eq 11 and the measured value of A_2. A diameter of 1.63 nm was found using eq 12. Equation 12 allows for smaller axial ratios than does eq 11. These values compare well to the value of 1.6 nm given by Russo et al.[24,38] (see Table II).

Dynamic Light Scattering. An example of the CONTIN DLS results from a binary PBLG/DMF solution is shown in the middle plot in Figure 7. The CONTIN data is presented as a plot of $G(R_h)$ vs R_h, where R_h is the "hydrodynamic radius" of the scattering species and is directly proportional to τ_R (eq 7) and inversely proportional to Γ. R_h was calculated from D using the Stokes–Einstein relation. The solvent viscosity was used in all cases to provide a standard for the comparison of all peaks. R_h is the actual radius only for spheres in pure solvent but provides a useful parameter for comparing peaks for all kinds of macromolecules. $G(R_h)$ is the distribution function representing the fraction of the scattered light from particles of "size" R_h.

Usually two peaks were seen in the CONTIN outputs. The dominant peak's frequency (Γ) scaled as q^2, so it was attributed to translation of the rods. The other appeared anywhere from 0.3 to 3 nm in R_h and never represented more than a couple percent of the total light scattered. Its position was too variable to say if it was angularly and/or concentration dependent. It did, however, appear at all concentrations and angles studied. It is likely this mode is due to translation–rotation coupling. For very long, thin rods in the dilute or semidilute regimes, a large anisotropy in the translational diffusion of the rod causes the otherwise independent translational and rotational motions of the rods to become coupled.[39] Theories taking this coupling into account predict a decay time (R_h) distribution consisting of two peaks instead of the usual one due to the translation of rods. This second peak had a smaller decay time than the first. For rods of length 70 nm, an apparent hydrodynamic radius of about 1 nm was estimated for this peak using the formulas given by Zero and Pecora,[39] well within the region where the peak was found experimentally. A weak third peak at a higher R_h than the translational diffusion mode was observed in 30% of the data at the highest concentration (30.2 mg/mL). This peak represented a maximum of 6% of the total scattered light intensity. Its position varied by up to a factor of 10 as the large R_h CONTIN window was widened also by a factor of 10. Because of its erratic behavior and low intensity, it is unlikely due to aggregation and is most probably due to dust. The variable behavior of this weak mode precluded comparisons to the slow modes observed in other rodlike systems.[10,24,40–43]

Table II
PBLG in DMF

ref	molecular weight, g/mol	A_2 ($\times 10^4$), cm^3 mol g^{-2}	k_D, cm^3/g	hydrodynamic diameter, nm	geometric diameter, nm
this work	102 000	3.9	See Table III	2.08	1.75[a]
					1.63[b]
Russo et al.[24]	179 000	3.1			
	300 000	3.1	11	2.0	1.6
Kubota and Chu[44]	268 000		6.9	2.2	
Kubota et al.[45]	299 000	3.1	17		1.4[a,b]
	372 000	3.3	18		1.5[a,b]
Schmidt[54]	560 000		33.5		
DeLong and Russo[38]	149 000	ave: 3.9			
	179 000				1.6
	277 000				

[a] Calculated from eq 11. [b] Calculated from eq 12.

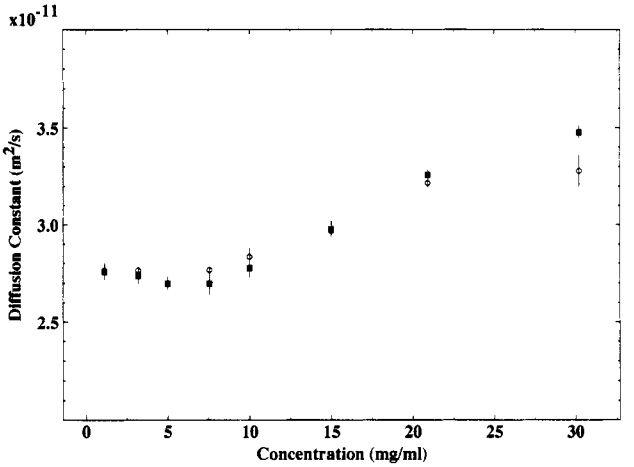

Figure 6. PBLG translational diffusion constant versus PBLG concentration in binary solutions from DLS. Data analyzed by the method of cumulants (○) and by CONTIN (■) are compared. Note the presence of two distinct concentration regimes. The break which occurs here at 8.4 mg/mL marks the change from the dilute to the semidilute regime.

The diffusion constants of PBLG in DMF are shown in Figure 6 as a function of concentration. Two regimes are clearly evident. The presence of these two distinct regimes has not been as clearly observed with PBLG by previous workers.[24,44,45] Qualitatively similar behavior, however, has been found in solutions of polystyrene coils[46,47] and in buffered solutions of polyadenylic acid.[48] For these solutions, the break in the slope was attributed to a transition between dilute and semidilute dynamics. Brown and Mortensen[46] noted that the transition concentration where overlap began was $c^* = 1/[\eta]$ where $[\eta]$ is the intrinsic viscosity. From PBLG viscosity data taken for this sample $[\eta] = 0.119 \pm 0.002$ mL/mg so $c^* = 8.4$ mg/mL ($nL^3 = 17$). The $[\eta]$ value compares well to data in Itou et al.[49] This c^* is very near where the transition occurs in Figure 6 (between 7.54 ($nL^3 = 15.2$) and 10.0 mg/mL ($nL^3 = 20$)). (The nL^3 values at all concentrations studied are shown in Table I.) This agrees with the Doi–Edwards[50–52] classification that semidilute behavior should begin at concentrations $c^* \gg M/L^3N_a = 0.5$ mg/mL for the PBLG used here. Moreover, Zero and Pecora[39] performed dynamic depolarized light scattering experiments on PBLG of molecular weights 150 000, 170 000, and 210 000 g/mol in dichloroethane and determined that the semidilute regime, as determined by a discontinuity in the rotational diffusion constant with concentration, began at a concentration of about 5 mg/mL. The semidilute regime in their study began at about $nL^3 = 21$, which is quite close to the transition point found here.

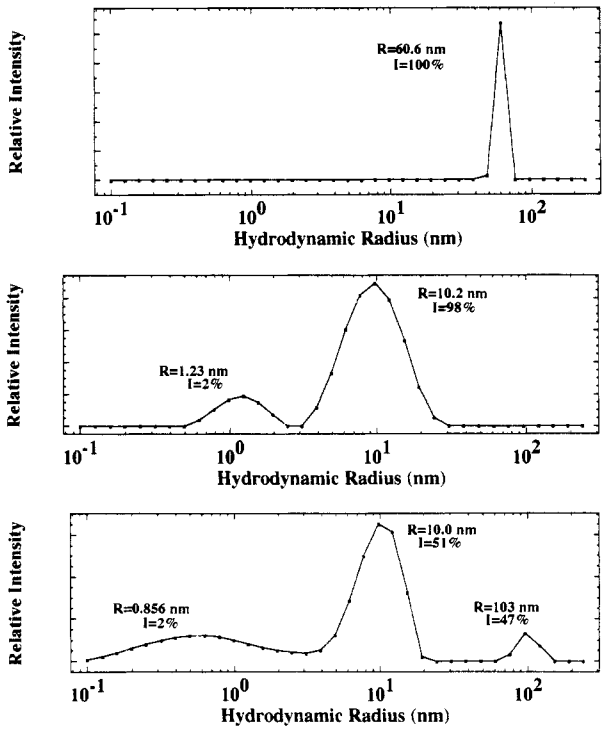

Figure 7. Comparison of binary solution DLS results to those of the ternary composite liquid. The top figure is a typical intensity versus hydrodynamic radius plot obtained from CONTIN for a 0.01% silica/DMF solution. Each CONTIN peak is marked by an R and an I. R is the average hydrodynamic radius of the peak and I is the fraction of the total scattered intensity within that peak. The second plot is a typical CONTIN output for a 0.5% PBLG/DMF solution. The bottom plot is a typical CONTIN output for the composite liquid showing both the rod and the sphere diffusion. This composite liquid contained 0.5% rods and 0.005% spheres in DMF. For each CONTIN output, the solvent viscosity, not the solution viscosity, was used to calculate R. This is why R for the sphere varies from the value in the sphere/DMF output. These examples were taken from data measured at 90°.

The two regimes were not so clearly observed before because all other DLS diffusion studies on PBLG found in the literature presented data that began at the end of the dilute regime so that only semidilute behavior was observed. As was noted for PBLG of molecular weights 300–400 000 g/mol, at $nL^3 < 20$ the solutions were so dilute that the scattered intensity is too weak to be detected and analyzed properly.[45] In previous studies of lower molecular weights, at most one data point was reported in the dilute regime. This is not enough to observe the trends seen here. In addition, this break in the diffusion coefficient between the dilute and semidilute regions was not seen in recent experiments on short (236 base pair) rodlike DNA fragments in 0.2 M NaCl possibly because

the concentration effect was so strong (k_D = 52 cm^3/g)[40] that the break in the diffusion versus concentration curve was too difficult to observe. Many more data points in the dilute region should be measured in the DNA system to better define the transition point. However, behavior similar to that found in our study was observed in 1 mM NaCl solutions of shorter (150 base pair) DNA fragments though this was attributed to the coupling of small ions with polyions.[41] Since PBLG has no net charge, this does not explain our results.

Below 10 mg/mL, the diffusion constant showed a very small decrease with concentration. However, this decrease is so slight that within the error the diffusion constant is essentially independent of concentration. Extrapolating the first four points to zero concentration gives an infinite dilution diffusion constant (D_0) of 2.77 ± 0.04 × 10^{-11} m^2/s. This value was used in the Broersma,[27-29] Tirado and Garcia de la Torre,[30] and Yamakawa and Fujii[53] models to determine the hydrodynamic diameter and rigidity of the rods. Broersma's result (eq 8) is generally considered to give the best fit for long rigid rods of $L/d > 5$, and the Tirado-Garcia de la Torre equation (eq 9) is generally considered to be most appropriate for shorter rigid rods in the range $2 < L/d < 30$. The Yamakawa-Fujii model pertains to semiflexible rods. PBLG diameters found by various experimental methods range from 1.36 to 2.2 nm,[49] so $32 < L/d < 51$ for this molecular weight. Thus, it might be expected that the Broersma equation would give the most consistent diameter in our case if the PBLG were rigid and rodlike. For a rod length of 70 nm and the measured D_0, all three equations were used to calculate the diameter. (It should be noted that Schmidt found the influence of polydispersity on the translational diffusion constant to be negligible if the weight average molecular weight was used to calculate the length.[54]) The hydrodynamic diameter was calculated to be 2.08 ± 0.8 nm using the Broersma equation. This compares well to the values found for PBLG of different molecular weights in DMF shown in Table II. The Tirado prediction for D_0 was on average 8% higher than the experimental value throughout the diameter range from 1.36 to 2.2 nm. Using the experimental D_0, a diameter of 2.76 nm was calculated using the Tirado equation which is well outside of the expected range. The Yamakawa–Fujii prediction was even worse. The D_0 calculated from the Yamakawa–Fujii equation over the experimental diameter range was 11% higher using a persistence length of 156.5 nm.[45] Changing the persistence length by up to 40% changed D_0 by only 0.5% maximum. The experimental error in D_0 is at most only 2.4%. Thus, both the total intensity and dynamic light scattering data show PBLG to be quite rigid at this molecular weight, unlike its behavior at higher molecular weights where the Yamakawa–Fujii prediction was found to be closest to the experimental results.[45] The hydrodynamic diameter was about 4 Å larger than the geometric diameter. This is possibly due to solvation effects in which DMF molecules (size about 4 Å) are carried along with the PBLG as it diffuses.[55]

In the second regime, there is a modest increase in the diffusion coefficient of PBLG with increasing concentration. This behavior has been previously observed by many investigators.[24,44,45,54] From a linear fit to the data in this regime (10 mg/mL and up), a zero-concentration intercept of D_0 = (2.46 ± 0.06) × 10^{-11} m^2/s was found (Table III). This value is 11.2% below D_0 determined from the dilute solution data only. Fitting all the data gave a 6.5% lower value for D_0. Thus, extrapolations of diffusion coefficient data to zero concentration often miss the changing slope in the dilute regime and give a smaller D_0 value than expected from the hydrodynamic models, as was found by Russo et al.[24] Using 2.59 × 10^{-11} m^2/s for D_0, a diameter of 2.58 ± 0.8 nm was calculated from Broersma's equation. This is 17% larger than the largest experimental value of 2.2 nm obtained from sedimentation data. Thus, values for D_0 obtained in this manner differ significantly from the value of (2.77 ± 0.04) × 10^{-11} m^2/s obtained above using only the low concentration data and lead to even larger discrepancies in the values calculated for the rod hydrodynamic diameter.

Table III
Linear Fits to the Rod Diffusion Data

	D_0,[a] ×10^{11} m^2/s	k_D(expt),[a] cm^3/g	k_f(expt),[b] cm^3/g
dilute regime (1.1–7.54 mg/mL)	2.77 ± 0.04	−4 ± 4	83 ● 5
semidilute regime	2.46 ± 0.06	14 ± 1	65 ± 3
all data	2.59 ± 0.02	11.0 ± 0.5	68 ± 3

[a] From fits to eq 13. [b] From eq 14.

Slopes were also calculated for the linear fits to the data. These are shown in Table III. From each slope and the intercept, values of k_D were determined according to eq 13.[24]

$$D = D_0(1 + k_D c) \tag{13}$$

The diffusion virial coefficient k_D is given by

$$k_D = 2MA_2 - k_f - \upsilon \tag{14}$$

where υ is the specific molar volume (0.791 cm^3/g for PBLG) and k_f is the coefficient in the linear term in the expansion of the friction factor in powers of the concentration.

As may be seen from the equations above, k_D is a measure of the competition between thermodynamic effects which, in the case of PBLG, speed up diffusion and frictional effects which slow it down.[24] A negative k_D means the enhanced friction due to the rod–rod interactions upon adding more rods is more important than the increased rod–rod repulsion due to crowding. A positive k_D means just the opposite while k_D = 0 indicates cancellation of these effects. In some cases an apparent negative k_D is indicative of aggregation.

Since eq 13 is valid at low concentrations where only pair correlations are significant, it is not surprising that this equation does not account for the change from negative to positive k_D seen here. Thus, we focus on the k_D values for each concentration regime rather than the overall value for the sake of comparison to other data in the literature. The k_D values reported here are compared to those obtained by other investigators for semidilute solutions of PBLG in DMF in Tables II and III. These values are about four times smaller than those found for semidilute solutions of charged, rodlike DNA of similar length.[40]

Equation 14 was used to determine the experimental k_f values for the different concentration regimes. The theoretical values for k_f given by Peterson[56] (eq 15) and Itou et al.[49] (eq 16) for a cylindrical hard rod at low concentration with the same molecular dimensions as found for PBLG of L = 70 nm are given in Table IV:

$$k_f = (RT/3\eta_0)(L^2/D_0M)(3d/8L)^{2/3} \tag{15}$$

$$k_f = (kT/3\eta_0)(3A_2N_a^{1/2}/2\pi)^{2/3}(M^{1/3}/D_0) \tag{16}$$

The k_f values calculated using eqs 15 and 16 are within the error identical to the experimental k_f values for the

Table IV
Comparison of Experimental and Theoretical Values of k_f and k_D

	k_D, cm³/g	k_f, cm³/g
experiment		
dilute	−4 ± 4	83 ± 5[a]
semidilute	14 ± 1	65 ± 3[a]
all data	11.0 ± 0.5	68 ± 3[a]
theory (Peterson)	−10 ± 5[d]	89 ± 4[b]
theory (Itou et al.)	−1 ± 3[e]	79 ± 1[c]

[a] k_f calculated from experimental k_D, A_2, and M values using eq 14. [b] k_f calculated from Peterson's equation (eq 15). [c] k_f calculated from Itou et al.'s equation (eq 16). [d] k_D calculated using the k_f value calculated from eq 15 and the experimental A_2 and M in eq 14. [e] k_D calculated using the k_f value calculated from eq 16 and the experimental A_2 and M in eq 14.

dilute regime. Such good agreement between theoretical and experiment values of k_f for rod systems has not been reported before. Peterson[56] found an error of 53% between his theory and the experimental value for dilute aqueous solutions of tobacco mosaic virus. Kubota et al.[45] reported a 20% error between experiment and theory for PBLG of molecular weights 290 000 and 372 000 g/mol. They attributed this to flexibility. Goinga and Pecora[40] also observed poor agreement between theory and experiment with semidilute aqueous solutions of DNA and attributed it to electrostatic interactions. Our results indicated that these equations are good approximations for stiff, uncharged rods at low concentrations.

The theories of Doi et al.[57-59] for the DLS dynamic structure factor of semidilute and concentrated solutions of long rigid rods gave neither qualitative nor quantitative descriptions of our DLS data even though the concentrations studied should fall within the range of their theory for semidilute solutions.[58] For instance, systematic deviations from q^2 dependence of the average decay rate were not observed. In addition, if the slower mode in our DLS results is identified with the D_{coop} of ref 58, k_D would, according to this theory be given by eq 14 with k_f and v set equal to zero. A perusal of Tables III and IV shows that this would give a much higher theoretical k_D than is measured in the semidilute region. This comparison uses the Doi–Edwards assumption that the rod self-diffusion coefficient in the semidilute region is concentration independent.[50-52] It is possible that this is not correct and a nonzero k_f could represent this dependence. However, according to Tables III and IV, k_f would have to be about 65 cm³/g to give agreement with experiment. DeLong and Russo[38] have obtained similarly poor agreement with the Doi et al.[58] theory for solutions of PBLG in DMF having even higher molecular weights than studied here. DeLong and Russo do not study the dilute behavior, but their studies spanned a wide range of the nondilute region.

CONTIN vs Cumulants. The rod/DMF and the rod/sphere/DMF data were analyzed by the method of cumulants in addition to CONTIN. The goal of this exercise was to get a better feel for when cumulants were good enough to accurately characterize a decay time distribution. It was found (to no surprise) that the cumulant results compared quite favorably to the CONTIN results when CONTIN showed one dominant peak as in the case of the rod/DMF solutions (Figure 6). However, if CONTIN showed two or more peaks, the two methods were no longer consistent. The normalized second cumulant (K_2/K_1^2) provided a good measure for determining whether or not the cumulant method was effective. Mustafa and Russo[2] found that if third order cumulants failed to fit the data, Laplace inversion was in order. They found this to be the case if $K_2/K_1^2 > 0.25$. The data here support this conclusion as this value ranged from 0.04 at the lowest concentration to 0.20 at the highest with values up to 0.25 found at the lowest angle of the least concentrated sample. This presumably was due to dust. Values for the composite liquid however varied from 0.25 at the lowest rod concentration to 0.8 at the highest one. So, at angles 60° or above, the data suggest that if $K_2/K_1^2 < 0.2$, cumulant and CONTIN results agreed within the error. If $0.2 \leq K_2/K_1^2 \leq 0.25$, agreement was likely but not certain, but if $K_2/K_1 > 0.25$, a more flexible method like CONTIN had to be used, as the results from CONTIN and the cumulants did not agree within the error. For example, $K_2/K_1^2 = 0.2$ for the highest concentration data point in Figure 6. Here the deviation from the CONTIN results first became significant. This was probably due to dust as discussed earlier.

Sphere/Solvent Studies. The concentration dependence of the coated monodisperse sphere diffusion coefficients in DMF was measured by DLS over the range used in the composite liquid experiments [0.053–0.32 mg/mL (0.005–0.03 mass %) silica]. Over this dilute concentration range, the diffusion constants were the same within experimental error. At higher polymer concentrations, higher concentrations of spheres were used so their scattering was commensurate with that of the rods as shown in Table I.

V. Composite Liquid DLS Results

CONTIN Peak Identification. The DLS results from the binary solutions (sphere/solvent and rod/solvent) may be compared with those from the composite liquids as shown in Figure 7. This comparison allows an unambiguous assignment of the composite liquid peaks given by CONTIN. In all the composite liquid data analyzed, at most two dominant peaks were resolved by CONTIN, depending on the solvent/sphere refractive index contrast.

The slow peak (large R_h) was attributed to the translational diffusion of the spheres in part because it was independent of angle and its frequency Γ scaled as q^2. Most importantly though, it was found that as the polymer concentration decreased, the hydrodynamic radius approached that of the spheres alone in DMF. Adding polymer increased the macroscopic viscosity of the solution, so the sphere diffusion slowed down as shown in Figure 12. Because the solvent viscosity (without rods or spheres) was always entered into CONTIN, CONTIN accounted for this decreased diffusion by increasing the variable R_h.

The faster peak (smaller R_h) was due to the translational diffusion of the rods. Again the corresponding diffusion constant was independent of angle and the frequency scaled with q^2, indicative of a diffusion process. The variation of the rod translational diffusion constant with polymer concentration closely follows that of the binary system confirming that the peak does belong to the rods. More importantly, this indicates that the spheres did not affect rod diffusion at these low sphere concentrations. The rod peak translational diffusion constant in the binary and ternary solutions is compared in Figure 8.

There is some deviation at the highest rod concentration, but this is due to the difficulty CONTIN has in fitting the rod peak because it decays very quickly on the time scale required to measure the relatively slow sphere diffusion as described earlier. Since relatively few data channels were used for the decay, the peak appears broadened especially toward the fast decay time edge of the window (small R_h). So the average diffusion constant calculated would be too high as observed.

The very fast, weak third peak that almost always appeared in the rod/DMF results again appears, though

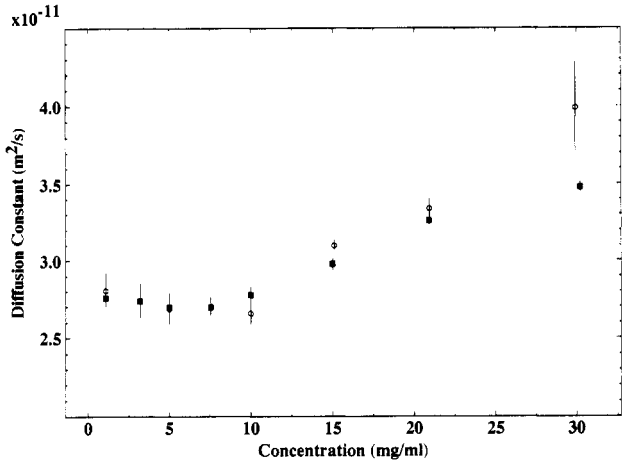

Figure 8. Rod translational diffusion constant versus concentration. The rod translational diffusion constants from the CONTIN results for the binary rod/DMF solutions (■) as compared to the rod diffusion constants from the CONTIN results for the composite liquids (○) at similar rod concentrations.

less frequently, in the composite liquid results. It appears in the same general region and has the same characteristics as in the binary system, though it is broader. It is most likely due to translational–rotational coupling of the rods.[39]

No diffusion slower than that of the spheres was observed, indicating the absence of large aggregates. However, at rod concentrations of 15 mg/mL and higher, a peak with a maximum intensity of 4% frequently appeared between the rod and sphere peaks. This weak peak's position was quite erratic, usually falling between 20 and 120 nm in R_h. Because of this variability, angular and concentration dependences could not be determined. Also, because of its low intensity, the peak rarely influenced the positions of the other peaks. As a result, it was thought to be merely an artifact.

Sphere Index Matching. An important advantage of this composite liquid system is that the sphere's contribution to the total light scattered can be reduced or eliminated by using a dimethylformamide/pyridine solvent mixture. Figure 9 shows that as the pyridine/DMF composition was raised to 31.8% pyridine, the sphere peak gradually disappeared while the rod peak remained. The experiments were done at a very low rod concentration (1.0 mg/mL) and a constant sphere concentration (0.047 mg/mL) similar to that used in the other composite liquid DLS studies. The low rod concentration was chosen so that the sphere would dominate the scattering and thus be more difficult to index match. In fact, the sphere peak went from contributing 80% of the scattered light intensity at 0% pyridine to 0% of the scattered light at 31.8% pyridine. Given this matching point, the Gladstone–Dale equation[60] for calculating the index of refraction of solvent mixtures gave an $n^{25}_D = 1.4528$. This compares quite well with other values for the refractive index of silica particles made by the Stöber process.[18,61] It should be noted that the rods were found to be both rigid and nonaggregating in these solvent mixtures. The spheres too were dispersible as singlets in the solvent mixtures.

The ability to match the spheres is quite useful. It provides another means for verifying which composite liquid peak belongs to the spheres. Since CONTIN is able to fit one peak more precisely than two, rod diffusion in the complex liquid can be studied more precisely than when the sphere peak is present. This would be particularly useful at polymer concentrations higher than those studied here. Incidentally, by adding more spheres away

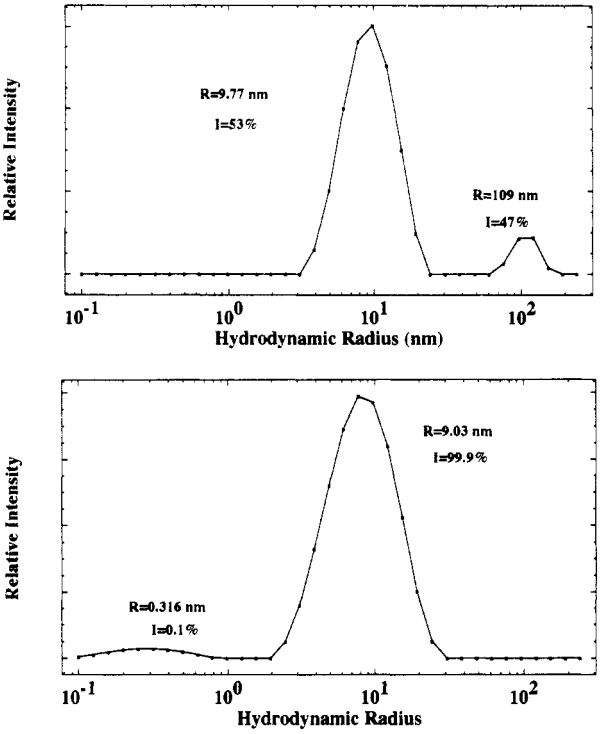

Figure 9. Sphere refractive index matching. The top plot shows the rod and sphere translational diffusion peaks in the CONTIN output for a solution of 0.5% rods and 0.005% spheres in pure DMF. The bottom figure shows the same thing for a solution of 0.1% rods and 0.005% spheres at the sphere matching point (31.8% pyridine/68.2% DMF). The sphere peak is gone.

from the matching point using either pure DMF or pyridine (where sphere scattering is up to 50% higher than in DMF), the contribution of the scattering due to the rods can be made virtually insignificant too. Most importantly though, the index matching allows solutions with a high concentration of spheres to be studied using optical techniques without complications due to multiple scattering and turbidity. For example, a solution of 34 mg/mL (3.5%) silica spheres was prepared in DMF and in DMF/pyridine at the matching composition. There the scattered light intensity at 90° was 100 times lower than in pure DMF. Furthermore, DLS results of this sample near the matching point measured at angles from 60° to 110° were identical to results of the dilute solutions of spheres in DMF discussed earlier.

Sphere Diffusion in the Complex Liquid. Another main goal of this study was to test the validity of the Stokes–Einstein relation for spheres in a nonaqueous solution of rodlike polymers. Figure 10 is a plot of the diffusion constant for the spheres obtained from CONTIN for each composite liquid sample versus the reciprocal of the macroscopic viscosity as measured by an Ostwald capillary viscometer. Figure 11 is another representation showing the variation of the data about the Stokes–Einstein prediction. The maximum deviation from the Stokes–Einstein prediction is only 6%. No coupling motions are seen here similar to those that have been noticed in a sphere/coil system and which caused a deviation to a higher D than predicted.[15,62] Thus, in the concentration range examined, the CONTIN results provide a good measure of the solution viscosity.

Langevin and Rondelez[63] have given a scaling argument to rationalize deviations from the Stokes–Einstein relation for diffusion of a particle of radius R through a semidilute solution of polymers. Their argument may be summarized

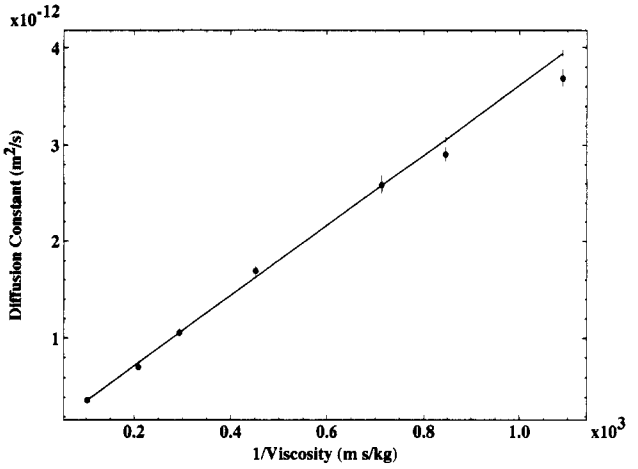

Figure 10. Stokes–Einstein behavior and sphere diffusion. The measured sphere diffusion constants in each composite liquid solution were plotted against the measured solution viscosity of the solutions (●). The line is determined from the theoretical diffusion constants calculated at each viscosity using the bare sphere radius 60.4 nm in the Stokes–Einstein equation.

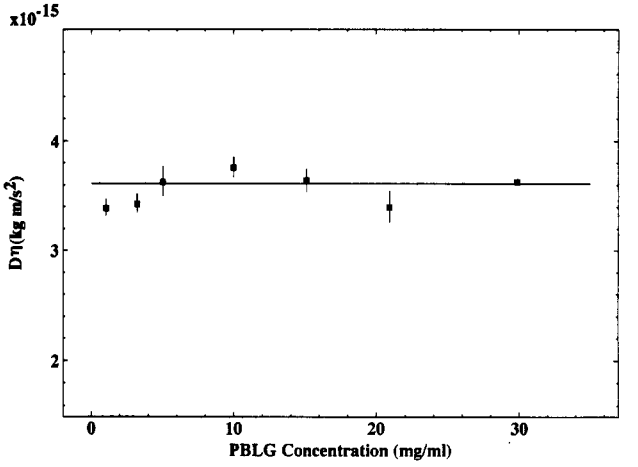

Figure 11. Deviation from the Stokes–Einstein equation. An alternative way of plotting the data in Figure 10 that shows the deviation (or lack thereof) more clearly is presented. Diffusion constants and viscosities were determined as in Figure 10. The line represents the expected results from the Stokes–Einstein law where $kT/6\pi R$ is constant at all concentrations.

by the following equation:

$$D/D_0 = \exp[-(R/\xi)] + \eta_0/\eta \tag{17}$$

where the subscript "0" indicates zero concentration of background polymer. In eq 17, ξ is the "correlation length" between molecules or cross-links. Four different methods were used to estimate ξ. The first equates it to the average distance between the centers of the rods assuming they are evenly spaced in the solution (ξ_c). ξ_c is calculated from eq 18,

$$\xi_c = \left(\frac{cN_a}{M}\right)^{-1/3} \tag{18}$$

and its values at various rod concentrations are listed in Table I. The second (ξ_r), used by Yang and Jamieson,[14] assumes that at the overlap concentration the molecules are a radius of gyration apart and ξ is inversely proportional to the polymer concentration:

$$\xi_r = r_g\left(\frac{c^*}{c}\right) \tag{19}$$

The third equates it to the static correlation length (ξ_s) measured from total intensity light scattering experiments.[38]

$$\frac{Kc}{R_\theta} = \frac{1}{RT}\left(\frac{\partial\pi}{\partial c}\right)_{TP}(1 + \xi_s^2 q^2) \tag{20}$$

K, c, R_θ, and q are as before and the derivative is the osmotic modulus. ξ_s is calculated from the slope and the intercept of a plot of $(Kc)/R_\theta$ versus q^2. The last estimate for ξ is the hydrodynamic correlation length (ξ_h) defined in terms of the Stokes–Einstein relation:

$$\xi_h = \frac{kT}{6\pi\eta_0 D} \tag{21}$$

where D is the diffusion coefficient of the polymer. Table I lists values for ξ obtained by all four methods.

According to eq 17, if $R > \xi$, the Stokes–Einstein relation holds as the sphere sees the macroscopic polymer solution viscosity η. But as R becomes less than ξ, D approaches D_0 as the sphere is able to diffuse in between polymers and thus sees an effective viscosity that approaches that of the pure solvent. The polymer concentrations were chosen such that ξ_c was on the order of the sphere radius. In these experiments in the semidilute regime, $2.4 < R/\xi_c < 3.4$. Moreover, $3.8 < R/\xi_r < 11.4$, $7.9 < R/\xi_s < 17.8$, and $6.2 < R/\xi_h < 7.7$ in the semidilute regime. Clearly, since no deviations from the Stokes–Einstein equation were observed, solutions with a much smaller R/ξ ratio must be studied to verify the predictions embodied in eq 17. It is important to note that Yang and Jamieson[14] found that eq 17 was valid only for $R/\xi_r > 5$ for polystyrene spheres in (hydroxypropyl)cellulose. In our system, with $\exp(-R/\xi)$ so small, it would be difficult to distinguish deviations from Stokes–Einstein behavior if they followed eq 17. Deviations from Stokes–Einstein behavior have not been observed in silica sphere/polymer systems studied by other workers either.[15,16,62] In these cases the background polymer was either polyisobutylene[15,62] (PIB) or poly(methacrylate)[16] (PMMA) in nonaqueous solvents. In these studies only ξ_h was determined and $3.3 < R/\xi_h < 45.6$ so that R/ξ was not less than 1 in these studies either.

Deviations from Stokes–Einstein behavior have been found in many non silica sphere/polymer systems. It has been determined that if diffusion is slower than Stokes–Einstein predicts, the polymer is likely adsorbing onto the spheres or causing sphere–sphere clustering.[2-6] Diffusion faster than predicted has also been observed, though exclusively in aqueous solutions of polystyrene spheres and a variety of polymers.[2,6-10,14] Phillies[7] noted that the Stokes–Einstein equation failed by up to a factor of 8 at large polymer molecular weights in the aqueous polystyrene/polymer systems. Interestingly, he found increasing R to 1–3 μm ($R \gg \xi$) did not improve the relation's validity. This is contrary to the prediction of Langevin and Rondelez[63] in eq 17. Yang and Jamieson[14] on the other hand observed deviations from the Stokes–Einstein relation as the polymer molecular weight increased and the radius of the sphere decreased qualitatively agreeing with eq 17. They also found a deviation of a factor of 100 in an aqueous system of polystyrene spheres and xanthan.[10] Though many have speculated on the reasons for the deviations from Stokes–Einstein behavior,[3] no satisfactory theory has yet been presented.

To summarize, no large magnitude deviations from Stokes–Einstein behavior have been observed in nonaqueous solutions of coil or rod polymers (as in that studied here). Large deviations have, however, been found, but not satisfactorily explained theoretically, in aqueous

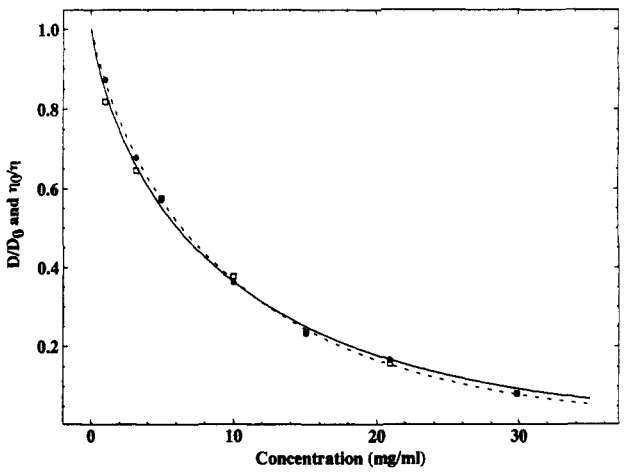

Figure 12. Stretched exponential fits to sphere diffusion constant and solution viscosity data as a function of concentration: □, the diffusion constant data; ●, the solution viscosity data. The solid line is the best fit to the diffusion data giving $\alpha = 0.17$ and $\nu = 0.77$. The dotted line is the best fit to the viscosity data given $\alpha = 0.15$, $\nu = 0.84$.

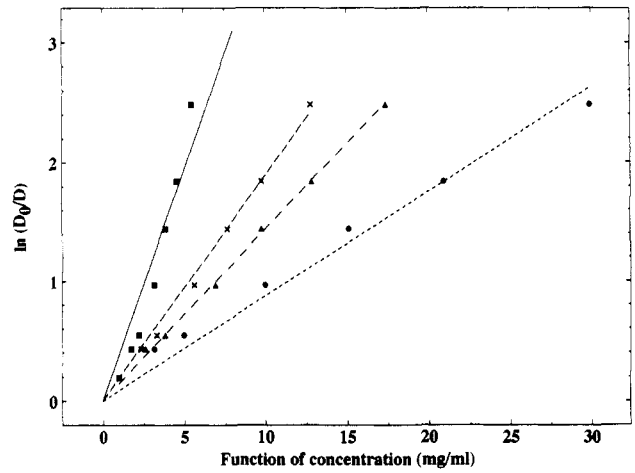

Figure 13. Exactness of the stretched exponential fit for concentration exponents (ν) between 0.5 and 1.0: ln (D_0/D) vs $c^{0.5}$ (■), vs $c^{0.75}$ (×), vs $c^{0.84}$ (▲), vs $c^{1.0}$ (●).

solutions of polystyrene spheres and coil or semiflexible polymers.

Models for Sphere Diffusion in Polymer Solutions. Probe diffusion has been found experimentally by many groups to follow a "stretched exponential" relationship between the sphere diffusion constant and the polymer concentration:[8,10-13]

$$D/D_0 = \exp(-\alpha c^{\nu}) \tag{22}$$

Since in this system the Stokes–Einstein equation is valid for the concentrations used, it would be expected that D and η^{-1} have the same concentration dependence. So the measured solution viscosity, η, should scale as

$$\eta/\eta_0 = \exp(\alpha c^{\nu}) \tag{23}$$

The experimental diffusion and viscosity data were fit to an exponential of the form $y = \exp(-\alpha x^{\nu})$ using a Marquardt fitting routine where α and ν are fitting parameters. These fits are shown in Figure 12. The following values were found: $\alpha_D = 0.17$, $\alpha_\eta = 0.15$, $\nu_D = 0.77$, $\nu_\eta = 0.84$. Excluding the D value for the $c = 1.0$ mg/mL, which was found to be furthest from the expected Stokes–Einstein value in Figure 10, gives $\alpha_D = 0.16$ and $\nu_D = 0.80$. Since this is a very flexible fitting function, further analysis was performed to obtain realistic error estimates for these parameters. The data were fit to a line through the origin by plotting ln (D_0/D) vs ln c^{ν} for $0.5 \leq \nu \leq 1.0$ as shown in Figure 13. The exactness of the fit (χ^2) for each line was compared to get an estimate of the error in the α and ν values obtained from the exponential fit. Values with conservative error estimates obtained by this procedure are $\alpha = 0.16 \pm 0.02$, $\nu = 0.81 \pm 0.07$. As expected, the diffusion and viscosity data have inverse concentration dependences. The value for ν is in accordance with the empirical prediction of Phillies for a polymer of molecular weight 102 000 g/mol.[8] This value also compares well to $\nu = 0.80$–0.85 found by Zhou and Brown for silica/PIB.[15] These results are lower than $\nu = 0.91$ found by Brown and Rymdén for silica/PMMA[16] and higher than the value of 0.62 found by Langevin and Rondelez for silica/poly(ethylene oxide).[63]

Several theories have been developed that predict an exponential dependence of D on concentration. Ogston et al.[64] examined the diffusion of large spheres through a suspension of long, rigid random fibers using a stochastic approach and found $\nu = 0.5$. Cukier also found $\nu = 0.5$ for both rod and coil polymers by using a hydrodynamic approach to model the effects of screening in semidilute polymer solutions.[65] Altenberger and Tirrell also predicted a $c^{0.5}$ dependence with a model where self-diffusion of a particle in a medium of fixed obstacles was used to simulate an entangled polymer network.[66] This model was generalized by examining the effects of statistical correlations in the placement of the fixed obstacles on the transport properties of particles through the network.[67] An exponent that fell between 0.5 and 1.0, depending on the hydrodynamic interactions between points in the polymer network and the concentration of obstacles, was obtained. At high concentration or strong hydrodynamic interactions, the c dependence is stronger than $c^{0.5}$.

Thus, not even theories that model the polymers as rigid rods[64-65] are able to exactly predict the experimentally determined concentration dependence of sphere diffusion in a rod solution. Since the deviation from $c^{0.5}$ behavior was found for solutions of rods and coils, this discrepancy is probably not due to polymer flexibility alone. The results of Altenberger et al.[67] suggest, however, that hydrodynamic interactions between the rods are important in characterizing sphere transport through a rod network. There is even less agreement on the theoretical significance of the parameter α which is often thought to depend in part on the sphere radius.[64,68] Current models are evidently inadequate to explain the diffusion of probe spheres in polymer/solvent systems.

VI. Conclusion

We have synthesized a new rod/sphere composite liquid and performed dynamic light scattering experiments to study the rod and sphere dynamics at a variety of concentrations. The diffusion of the rods in the composite liquid with dilute spheres was found to be identical to that in binary rod/DMF solutions. As the rod concentration is increased, two distinct diffusion regimes are observed. The transition point between these regimes occurred at 8.4 mg/mL, which agrees with the estimate of Doi and Edwards[50-52] and the experimental results of Zero and Pecora[39] for the transition region between the dilute and semidilute concentration regimes. The diffusion constant of the spheres was found to scale with the macroscopic viscosity of the solution in accordance with the Stokes–Einstein law. For the cases studied, the radius of the spheres was greater than the rod correlation length.

Langevin and Rondelez[63] have suggested that, in the semidilute region, deviations from Stokes–Einstein behavior of the spheres are likely to be seen when the sphere radius is less than the rod correlation length. For the current composite liquid, solutions of smaller spheres and larger molecular weight PBLG must be used to investigate this regime. Sphere diffusion for the dilute spheres was also shown to follow a stretched exponential relationship between the sphere diffusion constant and the rod concentration. A reciprocal relationship between the solution viscosity and the rod concentration was found, a further indication of Stokes–Einstein diffusion. Though the observed $c^{0.81}$ dependence differs from the theoretical $c^{0.5}$ dependence for spherical probes in a suspension of rods, it is similar to that found in silica sphere/coil polymer systems. Consequently, polymer flexibility alone does not adequately explain the differences between theory and experiment.

An important advantage of this rod/sphere system is its versatility. Since silica spheres can be synthesized from 10 nm up to almost 1 μm in diameter and PBLG of molecular weights 15 000–350 000 g/mol can be readily obtained, composite liquid dynamics can be studied over a wide range of component sizes. In addition, the sphere-matching procedure enables sphere concentrations over 3 orders of magnitude higher than those studied here to be investigated by DLS and other optical techniques such as transient electric birefringence. These features open the door for a wide variety of additional experiments like those described here as well as new experiments investigating, for example, rod rotational diffusion in confined environments and rheological properties in these liquids.

Acknowledgment. This work was supported by National Science Foundation Grant CHE-88-14641 to R.P. and by the NSF-MRL program through the Center for Materials Research at Stanford University. M.A.T. is greatly indebted to the United States Department of Education for financial support through the Graduate Assistance in Areas of National Need Progam (GAANN).

References and Notes

(1) National Research Council *Frontiers in Chemical Engineering*; National Academy Press: Washington, DC, 1988.
(2) Mustafa, M.; Russo, P. S. *J. Colloid Interface Sci.* **1989**, *129*, 240.
(3) Nehme, O. A.; Johnson, P.; Donald, A. M. *Macromolecules* **1989**, *22*, 4326.
(4) Russo, P. S.; Mustafa, M.; Cao, T.; Stephens, L. K. *J. Colloid Interface Sci.* **1988**, *122*, 120.
(5) Brown, W.; Rymdén, R. *Macromolecules* **1986**, *19*, 2942.
(6) Brown, W.; Rymdén, R. *Macromolecules* **1987**, *20*, 2867.
(7) Phillies, G. D. J.; Malone, C.; Ullmann, K.; Ullmann, G. S.; Rollings, J.; Yu, L.-P. *Macromolecules* **1987**, *20*, 2280.
(8) Phillies, G. D. J. *J. Phys. Chem.* **1989**, *93*, 5029.
(9) Gorthi, S.; Ware, B. R. *J. Chem. Phys.* **1985**, *83*, 6449.
(10) Jamieson, A. M.; Southwick, J. G.; Blackwell, J. *J. Polym. Sci.: Polym. Phys. Ed.* **1982**, *20*, 1513.
(11) Turner, D. N.; Hallett, F. R. *Biocheim. Biophys. Acta* **1976**, *451*, 305.
(12) Laurent, T. C.; Persson, H. *Biochim. Biophys. Acta* **1963**, *78*, 351.
(13) Phillies, G. D. J.; Ullmann, G. S.; Ullmann, K.; Lin, T.-H. *J. Chem. Phys.* **1985**, *82*, 5242.
(14) Yang, T.; Jamieson, A. M. *J. Colloid Interface Sci.* **1988**, *126*, 220.
(15) Zhou, P.; Brown, W. *Macromolecules* **1989**, *22*, 890.
(16) Brown, W.; Rymdén, R. *Macromolecules* **1988**, *21*, 840.
(17) Stöber, W.; Fink, A.; Bohn, E. *J. Colloid Interface Sci.* **1968**, *26*, 62.
(18) Van Helden, A. K.; Jansen, J. W.; Vrij, A. *J. Colloid Interface Sci.* **1981**, *81*, 354.
(19) Bogush, G. H.; Tracy, M. A.; Zukoski, C. F., IV *J. Non-cryst. Solids* **1988**, *104*, 95.
(20) Block, H. *Poly(γ-benzyl-L-glutamate) and Other Glutamic Acid Containing Polymers*; Gordon and Breach: New York, 1983; Chapter 5.
(21) Philipse, A.; Vrij, A. *J. Colloid Interface Sci.* **1989**, *128*, 121.
(22) Nishiyama, N.; Horie, K.; Asakura, T. *J. Colloid Interface Sci.* **1989**, *129*, 113.
(23) Bender, T. M.; Lewis, R. J.; Pecora, R. *Macromolecules* **1986**, *19*, 244.
(24) Russo, P. S.; Karasz, F. E.; Langley, K. H. *J. Chem. Phys.* **1984**, *80*, 5312.
(25) Berne, B. J.; Pecora, R. *Dynamic Light Scattering*; John Wiley and Sons: New York, 1976.
(26) Flamberg, A.; Pecora, R. *Macromolecules* **1988**, *88*, 3026.
(27) Broersma, S. *J. Chem. Phys.* **1960**, *32*, 1626.
(28) Broersma, S. *J. Chem. Phys.* **1960**, *32*, 1632.
(29) Broersma, S. *J. Chem. Phys.* **1981**, *74*, 6889.
(30) Garcia de la Torre, J.; López Martinez, M. C.; Tirado, M. M. *Biopolymers* **1984**, *23*, 611.
(31) Koppel, D. E. *J. Chem. Phys.* **1972**, *57*, 4814.
(32) Provencher, S. W. *Comput. Phys. Commun.* **1982**, *27*, 213.
(33) Provencher, S. W. *Comput. Phys. Commun.* **1982**, *27*, 229.
(34) Taylor, J. R. *An. Introduction to Error Analysis*; University Science Books: Mill Valley, CA, 1982.
(35) Fujita, H.; Teramoto, A.; Okita, K.; Yamashita, T.; Ikeda, S. *Bioplymers* **1966**, *4*, 769.
(36) Doty, P.; Bradbury, J. H.; Holtzer, A. M. *J. Amm. Chem. Soc.* **1956**, *78*, 947.
(37) Yamakawa, H. *Modern Theory of Polymer Solutions*; Harper and Row: New York, 1971; p 180–183.
(38) DeLong, L. M.; Russo, P. S. *Macromolecules*, in press.
(39) Zero, K. M.; Pecora, R. *Macromolecules* **1982**, *15*, 87.
(40) Goinga, H. Tj.; Pecora, R. *Macromolecules*, in press.
(41) Wang, L.; Garner, M. M.; Yu, H. *Macromolecules* **1991**, *24*, 2368.
(42) Nicoli, T.; Mandel, M. *Macromolecules* **1989**, *22*, 438.
(43) Nicoli, T.; Mandel, M. *Macromolecules* **1989**, *22*, 2248.
(44) Kubota, K.; Chu, B. *Biopolymers* **1983**, *22*, 1461.
(45) Kubota, K.; Tominaga, Y.; Fujime, S. *Macromolecules* **1986**, *19*, 1604.
(46) Brown, W.; Mortensen, K. *Macromolecules* **1988**, *21*, 420.
(47) Adam, M.; Delsanti, M. *Macromolecules* **1977**, *11*, 1229.
(48) Mathiez, P.; Mouttet, C.; Weisbuch, G. *Biopolymers* **1981**, *20*, 2381.
(49) Itou, S.; Nishioka, N.; Norisuye, T.; Teramoto, A. *Macromolecules* **1981**, *14*, 904.
(50) Doi, M. *J. Phys. (Paris)* **1975**, *36*, 607.
(51) Doi, M.; Edwards, S. F. *J. Chem. Soc., Faraday Trans. 2* **1978**, *74*, 560.
(52) Doi, M.; Edwards, S. F. *J. Chem. Soc., Faraday Trans. 2* **1978**, *74*, 918.
(53) Yamakawa, H.; Fujii, M. *Macromolecules* **1973**, *6*, 407.
(54) Schmidt, M. *Macromolecules* **1984**, *17*, 553.
(55) Venable, R. M.; Pastor, R. W. *Biopolymers* **1988**, *27*, 1001.
(56) Peterson, J. *J. Chem. Phys.* **1964**, *40*, 2680.
(57) Shimada, T.; Doi, M.; Okano, K. *J. Chem. Phys.* **1988**, *88*, 2815.
(58) Doi, M.; Shimada, T.; Okano, K. *J. Chem. Phys.* **1988**, *88*, 4070.
(59) Shimada, T.; Doi, M.; Okano, K. *J. Chem. Phys.* **1988**, *88*, 7181.
(60) *Light Scattering From Polymer Solutions*; Huglin, M. B., Ed.; Academic Press: London, 1972.
(61) Philipse, A. P.; Smits, C.; Vrij, A. *J. Colloid Interface Sci.* **1989**, *129*, 335.
(62) Zhou, P.; Brown, W. *Macromolecules* **1989**, *22*, 4031.
(63) Langevin, D.; Rondelz, F. *Polymer* **1978**, *19*, 875.
(64) Ogston, A. G.; Preston, B. N.; Wells, J. D. *Proc. R. Soc. London A* **1973**, *333*, 297.
(65) Cukier, R. I. *Macromolecules* **1984**, *17*, 252.
(66) Altenberger, A. R.; Tirrell, M. *J. Chem. Phys.* **1984**, *80*, 2208.
(67) Altenberger, A. R.; Tirrell, M.; Dahler, J. S. *J. Chem. Phys.* **1986**, *84*, 5122.
(68) Phillies, G. D. J. *Macromolecules* **1988**, *21*, 3101.

Registry No. PBLG (homopolymer), 25014-27-1; PBLG (SRU), 25038-53-3; TPM, 2530-85-0; SiO_2, 7631-86-9.